

# Push–Pull Type Oligo(*N*-annulated perylene)quinodimethanes: Chain Length and Solvent-Dependent Ground States and Physical Properties

Zebing Zeng,<sup>†,‡</sup> Sangsu Lee,<sup>§</sup> Minjung Son,<sup>§</sup> Kotaro Fukuda,<sup>||</sup> Paula Mayorga Burrezo,<sup>⊥</sup> Xiaojian Zhu,<sup>#</sup> Qingbiao Qi,<sup>†</sup> Run-Wei Li,<sup>#</sup> Juan T. López Navarrete,<sup>⊥</sup> Jun Ding,<sup>\*,∇</sup> Juan Casado,<sup>\*,⊥</sup> Masayoshi Nakano,<sup>\*,||</sup> Dongho Kim,<sup>\*,§</sup> and Jishan Wu<sup>\*,†</sup>

<sup>†</sup>Department of Chemistry, National University of Singapore, 3 Science Drive 3, Singapore 117543, Singapore

<sup>‡</sup>State Key Laboratory of Chemo/Biosensing and Chemometrics, College of Chemistry and Chemical Engineering, Hunan University, Changsha 410082, People's Republic of China

<sup>§</sup>Spectroscopy Laboratory for Functional  $\pi$ -Electronic Systems and Department of Chemistry, Yonsei University, Seoul 120-749, Korea

<sup>||</sup>Department of Materials Engineering Science, Graduate School of Engineering Science, Osaka University, Toyonaka, Osaka 560-8531, Japan

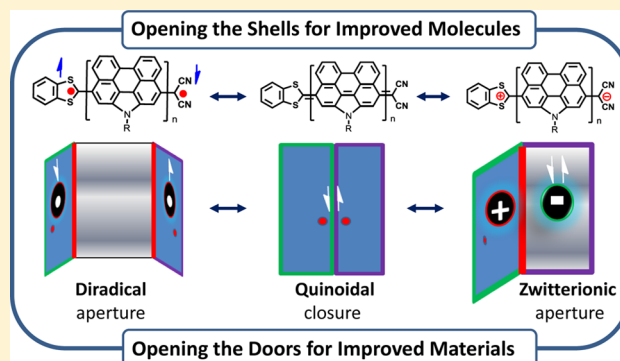
<sup>⊥</sup>Department of Physical Chemistry, University of Málaga, Campus de Teatinos s/n, 229071 Málaga, Spain

<sup>#</sup>Key Laboratory of Magnetic Materials and Devices, Ningbo Institute of Materials Technology and Engineering, Chinese Academy of Sciences, Ningbo 315201, People's Republic of China

<sup>∇</sup>Department of Materials Science & Engineering, National University of Singapore, Singapore 119260, Singapore

## Supporting Information

**ABSTRACT:** Research on stable open-shell singlet diradicaloids recently became a hot topic because of their unique optical, electronic, and magnetic properties and promising applications in materials science. So far, most reported singlet diradicaloid molecules have a symmetric structure, while asymmetric diradicaloids with an additional contribution of a dipolar zwitterionic form to the ground state were rarely studied. In this Article, a series of new push–pull type oligo(*N*-annulated perylene)quinodimethanes were synthesized. Their chain length and solvent-dependent ground states and physical properties were systematically investigated by various experimental methods such as steady-state and transient absorption, two-photon absorption, X-ray crystallographic analysis, electron spin resonance, superconducting quantum interference device, Raman spectroscopy, and electrochemistry. It was found that with extension of the chain length, the diradical character increases while the contribution of the zwitterionic form to the ground state becomes smaller. Because of the intramolecular charge transfer character, the physical properties of this push–pull system showed solvent dependence. In addition, density functional theory calculations on the diradical character and Hirshfeld charge were conducted to understand the chain length and solvent dependence of both symmetric and asymmetric systems. Our studies provided a comprehensive understanding on the fundamental structure– and environment–property relationships in the new asymmetric diradicaloid systems.



## I. INTRODUCTION

Conjugated polycyclic hydrocarbons (PHs) with an open-shell singlet ground state have recently attracted a great deal of attention not only from theoreticians but also from experimentalists.<sup>1</sup> Fundamentally, the studies extend the concept of “chemical bonding” by realizing flexible chemical bonds, multicenter bonds, associated with intermediate or strong electron correlations. Practically, this type of open-shell  $\pi$ -conjugated diradicaloids shows unique optical, electronic, and

magnetic properties and have many potential applications for organic electronics, photonics, spintronics, and energy storage devices.<sup>2</sup> It is thus critical to clarify the fundamental relationships between the molecular structures, the electronic, optical, and magnetic properties, and the diradical character. So far, various stable open-shell singlet PHs have been theoretically

Received: April 22, 2015

Published: June 11, 2015

and experimentally investigated, including bis(phenalenyls),<sup>3</sup> zethrenes,<sup>4</sup> indenofluorenes,<sup>5</sup> extended *p*-quinodimethanes (*p*-QDMs),<sup>6</sup> and zigzag edged graphene molecules.<sup>7</sup> It has been demonstrated that aromaticity, steric repulsion, and substitution all play important roles in determining the nature of the ground state and the diradical character.<sup>1</sup> Open-shell singlet compounds with a moderate diradical character index ( $\gamma$ ) usually exhibit larger second hyperpolarizabilities  $\gamma$  than the closed-shell and pure diradical molecules with similar conjugation length, the feature of which was first predicted by theory<sup>8</sup> and then substantiated by experiments,<sup>2c,4,6,9</sup> and thus represent a novel class of nonlinear optical (NLO) chromophores.<sup>8j</sup> In addition, a small singlet–triplet energy gap ( $\Delta E_{S-T} < 6$  kcal/mol) is normally observed in these open-shell systems, which allows for a thermal promotion of the singlet to triplet state and resulted in unique magnetic properties. In particular, these compounds are expected to be good charge and spin transporting materials in spin-based electronics.

Among various classes of open-shell singlet PHs, *p*-QDM is a fundamental pro-aromatic building block, which can be drawn in a closed-shell quinoidal resonance form and an open-shell diradical resonance form (Figure 1). Because of the gain of

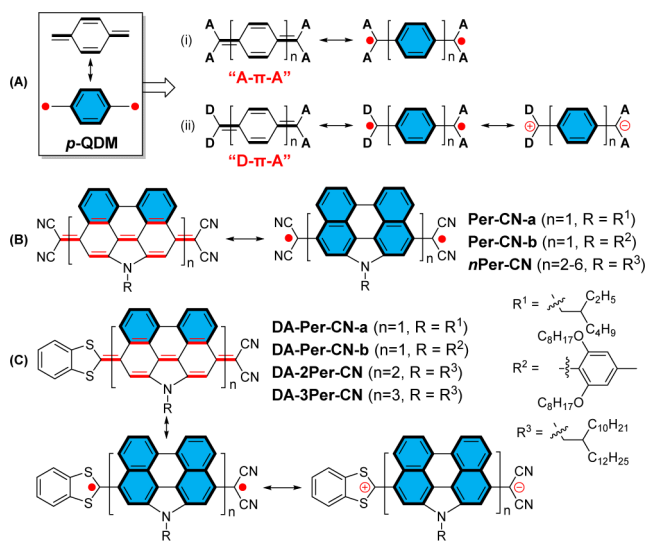


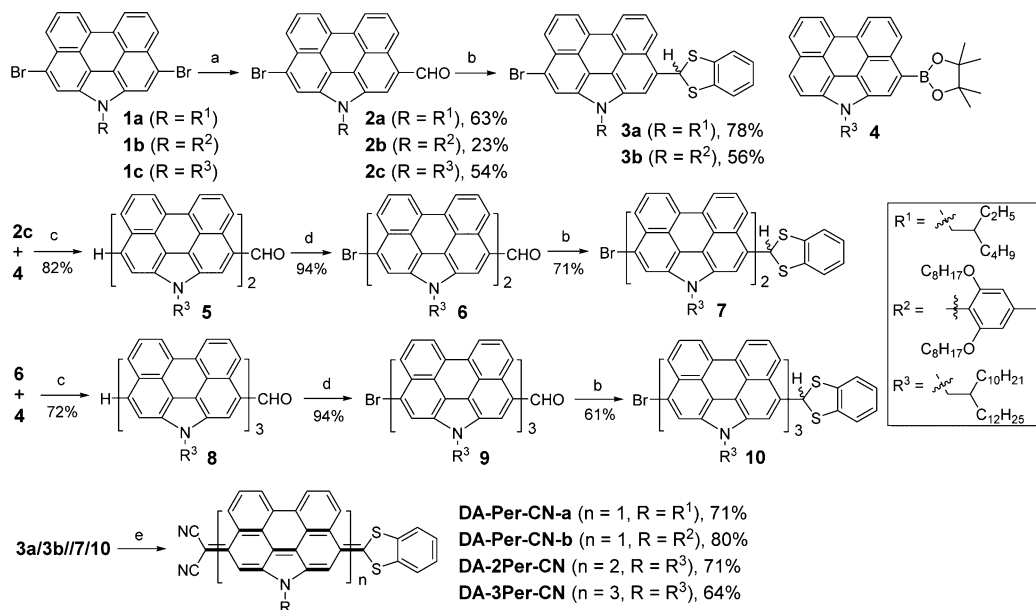
**Figure 1.** Chemical and resonance structures of pull–pull and push–pull type *p*-QDMs (A), and pull–pull (B)/push–pull (C) type oligo(*N*-annulated perylene) quinodimethanes.

additional aromatic sextet rings (highlighted in blue color) in the diradical form, *p*-QDM shows a large diradical character and thus is highly reactive.<sup>10</sup> Making extended *p*-QDMs or incorporation of *p*-QDM moiety into a polycyclic aromatic hydrocarbon framework are the two general strategies to obtain a PH with an open-shell singlet ground state. However, one key issue is how to stabilize the highly reactive diradical species. One general method to stabilize the reactive *p*-QDM and extended *p*-QDMs is to attach phenyl groups to the methylene termini via resonance effect (e.g., in Thiele’s<sup>11</sup> and Tschitschibabin’s<sup>12</sup> hydrocarbons) or strong electron-withdrawing groups such as cyano- groups (e.g., 7,7,8,8-tetracyanoquinodimethane (TCNQ)<sup>15</sup>), leading to a pull–pull (or A– $\pi$ –A) type structure (Figure 1). The efficiency of this approach however is limited by the poor solubility and still-high reactivity of longer oligomers.<sup>14</sup> Alternatively, heterocycles such as thiophene with smaller aromatic resonance energy than

benzene were incorporated and resulted in stable quinoidal oligothiophenes and thienoacenes with distinct diradical characters, which also showed interesting ambipolar or *n*-type charge transporting behavior.<sup>15</sup> We recently demonstrated that benzannulation is another strategy to stabilize the highly reactive extended *p*-QDMs.<sup>6b</sup> In particular, a series of tetracyano-oligo(*N*-annulated perylene (NP))-quinodimethanes *nPer-CN* ( $n = 1–6$ ) (Figure 1) have been synthesized, which exhibited chain length-dependent tunable ground states and physical properties.<sup>6c</sup> In general, the diradical character increases with the increase of the chain length due to the large steric repulsion between the NP units and the gain of aromaticity of the NP moieties in the diradical form. On the other hand, the planarized quinoidal rylene displayed much smaller diradical characters as compared to the respective unfused oligomers,<sup>6d</sup> but it was tunable by incorporation of additional thiophene units.<sup>6e</sup>

So far, most of the experimentally investigated open-shell singlet diradicaloids are symmetric molecules. Theoretically, Nakano et al. predicted that the asymmetric open-shell singlet systems with intermediate diradical characters can exhibit further enhancements of static first and second hyperpolarizabilities as compared to conventional asymmetric closed-shell systems and also to symmetric open-shell singlet systems with intermediate diradical character,<sup>16</sup> which however has not been experimentally validated due to the lack of such asymmetric open-shell system. Incorporation of electron-donating (D) and electron-accepting (A) groups into the extended *p*-QDMs is thus a reasonable strategy to generate asymmetric open-shell singlet diradicaloids with a push–pull (or D– $\pi$ –A) type structure, and contribution of a dipolar zwitterionic resonance form has to be considered in this case (Figure 1). In fact, push–pull type *p*-QDM,<sup>17</sup> *p*-diphenoquinodimethane,<sup>18</sup> and their heterocyclic analogues<sup>19</sup> have been synthesized and exhibited strong intramolecular charge transfer and long-wavelength absorption in the near-infrared (NIR) region. However, none of them exhibited an open-shell singlet ground state.

In this context, we are interested in developing the first push–pull type open-shell diradicaloid system by using the quinoidal NP and its oligomers as the spacers (Figure 1). The two terminal sites were substituted by benzo-1,3-dithiol-2-ylidene (donor) and dicyanomethylene (acceptor), respectively. DA-Per-CN-a and DA-Per-CN-b represent the smallest derivatives with different substituents at the amine-site (vide infra), while DA-2Per-CN and DA-3Per-CN are the higher order analogues. These  $\pi$ -extended push–pull chromophores are expected to show unique chain length and solvent-dependent ground states, and it is of interest to understand the contribution of each resonance structure (a closed-shell quinoidal form, an open-shell diradical form, and a closed-shell zwitterionic form) to the ground state (Figure 1) and the consequence in view of their physicochemical properties. In this Article, we report the detailed studies on their synthesis, their chain length, and solvent-dependent ground-state electronic structures and physical properties through a systematic experimental analysis by steady-state one-photon absorption (OPA), transient absorption (TA), two-photon absorption (TPA), X-ray crystallographic analysis, variable temperature (VT) electron spin resonance (ESR), superconducting quantum interference device (SQUID) measurements, FT Raman spectroscopy, and electrochemistry. Density functional theory (DFT) calculations were conducted to calculate the

Scheme 1. Synthesis of Push–Pull Type Quinoidal NP Oligomers DA-Per-CN-a/b, DA-2Per-CN, and DA-3Per-CN<sup>a</sup>

<sup>a</sup>Reagents and conditions: (a) (i) *n*-BuLi, THF,  $-78\text{ }^\circ\text{C}$ , 2 h; (ii) DMF,  $-78\text{ }^\circ\text{C}$ –rt, 4 h; (iii) sat.  $\text{NH}_4\text{Cl}$ ; (b) 1,2-benzenedithiol, *p*-toluenesulfonic acid monohydrate, toluene, reflux, overnight; (c)  $\text{Pd}(\text{PPh}_3)_4$ ,  $\text{K}_3\text{PO}_4$ , toluene/DMF,  $80\text{ }^\circ\text{C}$ , 48 h; (d) NBS (1 equiv), DCM/DMF,  $0\text{--}25\text{ }^\circ\text{C}$ , overnight; (e) (i) malononitrile, NaH,  $\text{Pd}(\text{PPh}_3)_4$  or  $\text{Pd}(\text{PPh}_3)_2\text{Cl}_2$ , dppf, THF, reflux, 48 h; (ii) HCl (2 M), air; (iii) silica gel, *p*-chloranil, DCM, rt.

diradical character and Hirshfeld, which assist us to explain the experimental observations. Our studies provide a comprehensive understanding on the fundamental structure– and environment–property relationships for the unique push–pull type open-shell singlet diradicaloid system.

## II. RESULTS AND DISCUSSION

**1. Synthesis.** The push–pull type quinoidal NP oligomers were prepared mainly by Pd-catalyzed Takahashi coupling<sup>20</sup> from the corresponding bromo- and benzo-1,3-dithiol-2-yl-substituted oligo(*N*-annulated perylenes) 3/7/10, followed by oxidative dehydrogenation (Scheme 1). This chemistry proceeded most cleanly with catalyst of  $\text{Pd}(\text{PPh}_3)_4$ /dppf complex for monomer, but with  $\text{Pd}(\text{PPh}_3)_2\text{Cl}_2$ /dppf for dimer DA-2Per-CN and trimer DA-3Per-CN. The monomer was synthesized starting from dibromo-NP 1 with short alkyl substituent 2-ethylhexyl (1a)<sup>6c</sup> or bulky substituent 2,6-dioctyloxytolyl (1b).<sup>21</sup> Treatment of 1 with 1 equiv of *n*-butyl lithium in THF at  $-78\text{ }^\circ\text{C}$  followed by reacting with anhydrous DMF converted one of the two bromo groups into aldehyde and gave the asymmetric formyl-substituted monobromo-NP 2a/b after acidification, which was subjected to thioacetal formation with 1,2-benzenedithiol to afford the key intermediate 3a/b. Finally, the Pd(0)/dppf complex-catalyzed coupling reaction between 3a/b and malononitrile in the presence of sodium hydride in anhydrous THF afforded the monomer DA-Per-CN-a/b as a green solid in good yields (70–80%) after acidification and immediate oxidation with a catalytic amount of *p*-chloranil on silica gel. Unlike the symmetric Per-CN-a with good solubility in normal organic solvents, the asymmetric compound DA-Per-CN-a showed very poor solubility and significantly broadened NMR spectrum due to strong intermolecular dipole–dipole and  $\pi$ – $\pi$  interactions (vide infra). More seriously, a very long tail extending to 1500 nm was observed in the absorption spectrum (Figure S1 in the Supporting Information), which made the

two-photon absorption measurements of this compound difficult because the TPA excitation wavelength overlaps with this one-photon absorption band. To solve these problems, a bulky 2,6-dioctyloxytolyl group was attached to the amine-site in DA-Per-CN-b, which turned out to be a very efficient way to suppress dye aggregation.<sup>21</sup> For comparison, a new pull–pull type quinoidal Per-CN-b with the same bulky substituent was also prepared (see the Supporting Information). For the longer oligomers, long branched dove-tailed chains (2-decyltetradecyl) were introduced to the *N*-sites to ensure sufficient solubility for the intermediates and the final products. The same approach starting from the symmetric dibromo-NP dimer<sup>6c</sup> was attempted for the synthesis of formyl-substituted monobromo-dimer 6, but the reaction was unsuccessful. Alternatively, the formyl-substituted NP dimer 5 was first synthesized by Suzuki coupling between the NP monoboronic ester 4<sup>6c</sup> and 2c (prepared by a similar approach from 1c), and subsequent bromination at another terminal *peri*-position of NP unit gave compound 6. The key intermediate 7 was then successfully prepared by thioacetalization of 6. Similar Suzuki coupling/bromination/thioacetalization protocol from 6 generated the formylated NP trimer 8, the brominated formyl-NP trimer 9, and the key intermediate 10. Finally, the push–pull type quinoidal NP dimer DA-2Per-CN and trimer DA-3Per-CN were prepared by similar Takahashi coupling reaction from the corresponding bromo- and benzo-1,3-dithiol-2-yl-substituted dimer and trimer (7 and 10) followed by oxidation with *p*-chloranil in 71% and 64% yield, respectively. During the workup, the dihydro- intermediates were only partially oxidized in air, and thus a stronger oxidant such as *p*-chloranil has to be used to ensure a complete dehydrogenation. All of the target compounds are stable enough both in solution and in solid states. All of the intermediates and final products were well characterized by  $^1\text{H}$  and  $^{13}\text{C}$  NMR and high-resolution mass spectrometry (MS), and the purity of the final products was

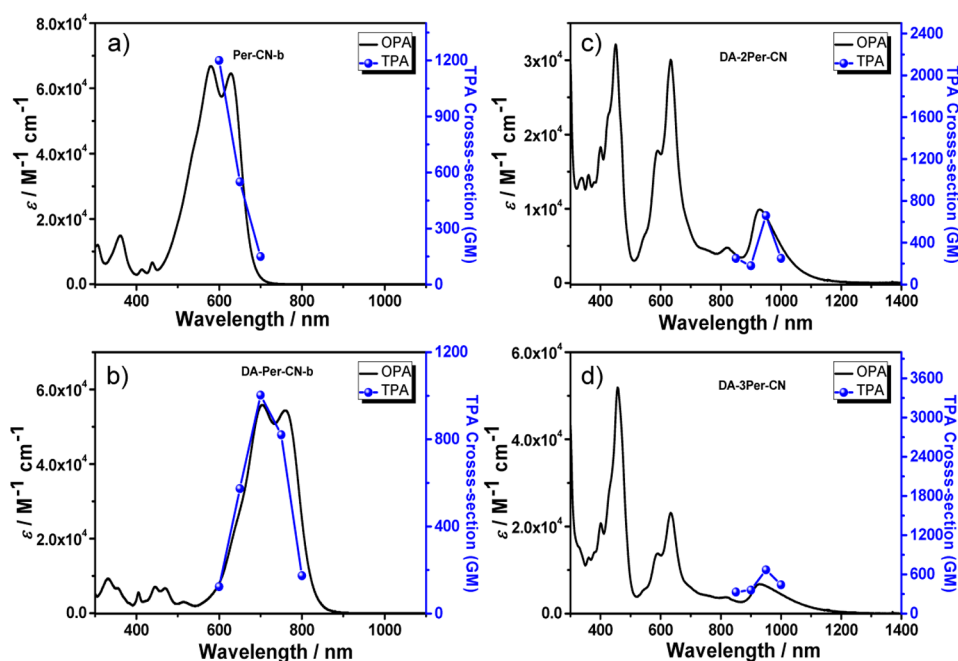


**Figure 2.** One-photon and two-photon absorption spectra of (a) Per-CN-b, (b) DA-Per-CN-b, (c) DA-2Per-CN, and (d) DA-3Per-CN. The spectra were recorded in DCM. TPA spectra are plotted at  $\lambda_{\text{ex}}/2$ .

**Table 1. Photophysical and Electrochemical Data of Per-CN-b, DA-Per-CN-b, DA-2Per-CN, and DA-3Per-CN<sup>a</sup>**

compd	$\lambda_{\text{abs}}$ (nm)	$\epsilon_{\text{max}}$ ( $\text{M}^{-1}\text{cm}^{-1}$ )	$\tau$ (ps)	$\sigma_{\text{G}}^{(2)\text{max}}$ (GM)	$E_{1/2}^{\text{ox}}$ (V)	$E_{1/2}^{\text{red}}$ (V)	HOMO (eV)	LUMO (eV)	$E_{\text{g}}^{\text{EC}}$ (eV)	$E_{\text{g}}^{\text{opt}}$ (eV)	$\Delta E_{\text{S-T}}$ (kJ/mol)
Per-CN-b	579	67 100	3, 12	1400 (a)		-1.38		-4.26		1.82	
	629	65 000				-0.78					
						-0.54					
DA- Per- CN-b	704	55 900	1.3	1000 (b)	0.32	-1.02	-5.06	-3.85	1.21	1.36	
	760	54 300			0.78						
DA- 2Per- CN	450	32 100	12.8	660 (c)	0.31	-1.38	-5.06	-4.46	0.60	0.96	-1.46
	633	30 100			0.47	-1.12					
	929	9900			0.83	-0.40					
DA- 3Per- CN	457	51 900	15.0	670 (c)	0.32	-1.40	-5.02	-4.52	0.50	0.95	-0.48
	634	23 100			0.49	-1.16					
	926	6800			0.60	-0.40					
					0.76	-0.40					
					0.89						

<sup>a</sup> $\lambda_{\text{abs}}$ : absorption maximum.  $\epsilon_{\text{max}}$ : molar extinction coefficient at the absorption maximum in the unit of  $\text{M}^{-1}\text{cm}^{-1}$ .  $\tau$  is singlet excited-state lifetime obtained from TA in toluene.  $\sigma_{\text{G}}^{(2)\text{max}}$  is the maximum TPA cross-section at the wavelength of: (a) 1200 nm, (b) 1500 nm, and (c) 1900 nm, measured in DCM.  $E_{1/2}^{\text{ox}}$  and  $E_{1/2}^{\text{red}}$  are half-wave potentials of the oxidative and reductive waves, respectively, with potentials vs Fc/Fc<sup>+</sup> couple. HOMO and LUMO energy levels were calculated according to equations: HOMO =  $-(4.8 + E_{\text{ox}}^{\text{onset}})$  and LUMO =  $-(4.8 + E_{\text{red}}^{\text{onset}})$ , where  $E_{\text{ox}}^{\text{onset}}$  and  $E_{\text{red}}^{\text{onset}}$  are the onset potentials of the first oxidative and reductive redox wave, respectively.  $E_{\text{g}}^{\text{EC}}$ : electrochemical energy gap derived from LUMO–HOMO.  $E_{\text{g}}^{\text{opt}}$ : optical energy gap derived from the lowest energy absorption onset in the absorption spectra.  $\Delta E_{\text{S-T}}$ : singlet–triplet energy gap estimated from SQUID measurements.

further confirmed by high performance liquid chromatography (HPLC) (see the Supporting Information).

## 2. Chain Length-Dependent Ground States and Physical Properties. 2.1. Electronic Absorption Spectra.

All of the push–pull type NP monomers and oligomers were deeply colored in both solid and solution phases. Their OPA spectra in dichloromethane (DCM) are shown in Figure 2, and the data are summarized in Table 1. Unlike the *N*-2-ethylhexyl-substituted monomer DA-Per-CN-a, which displays a long absorption tail to the NIR region due to strong aggregation in solution, the bulky *N*-2,6-dioctoxytolyl substituted monomer DA-Per-CN-b shows an intense absorption band with two peaks at 704 and 754 nm without any tailing to the NIR region,

implying a successful suppression of dye aggregation, which is also supported by the observed sharp <sup>1</sup>H NMR spectrum (Supporting Information). The band structure resembles that of the pull–pull type monomer Per-CN-b, indicating that both have the same closed-shell quinoidal ground state. The spectrum however exhibits a red shift of about 125 nm in comparison to the Per-CN-b due to the intramolecular charge transfer character in this push–pull type structure. The absorption spectrum of push–pull type dimer DA-2Per-CN suddenly changed, which consists of three major absorption bands with maxima at 450, 633, and 929 nm, respectively. The longest-wavelength absorption band was observed in the NIR region extending up to 1290 nm, with a very small optical

energy gap of 0.96 eV. Such a band structure is very similar to that of the previously reported pull–pull type trimer **3Per-CN**, which has an open-shell singlet ground state with a large diradical character ( $y = 0.99$ ), but different from that of the symmetric dimer **2Per-CN** with a smaller diradical character ( $y = 0.85$ ).<sup>6c</sup> This observation suggests that, as compared to the pull–pull type symmetric oligomers with the same conjugation length, the NP units in the push–pull type oligomers display larger aromatic character due to the joint contributions of the diradical form and zwitterionic form to the ground state. Passing from dimer to trimer, **DA-3Per-CN** also demonstrated three major absorption bands in the region from 400 to 1305 nm, with maximum at 457, 634, and 926 nm, respectively. The relative intensity of the band at 457 nm for the aromatic NP units increases due to more NP units in the trimer. The evolution of the characteristic bands in these push–pull type molecules is similar to that of pull–pull type oligomers *nPer-CN*s, and we can conclude that with extension of the chain length, the contribution of the closed-shell quinoidal form to the ground-state electronic structure becomes gradually smaller. The major reason should be the same; that is, the longer oligomers tend to exist as a flexible diradical/zwitterionic form rather than as a highly strained quinoidal form. However, we are not able to conclude on the diradical character and zwitterionic character just based on the absorption spectrum at this stage (see more detailed analysis in the coming sections).

**2.2. Magnetic Properties.** The ground states of these new push–pull type oligomers were further investigated by magnetic measurements such as VT NMR, ESR, and SQUID measurements. The <sup>1</sup>H and <sup>13</sup>C NMR spectrum of **DA-Per-CN-b** in CDCl<sub>3</sub> exhibited sharp peaks at room temperature and even at elevated temperature, confirming its closed-shell nature of the ground state. In contrast, the higher series **DA-2Per-CN** and **DA-3Per-CN** showed NMR silence even at the low temperature (e.g., −100 °C), implying that they have an open-shell diradical ground state with a large diradical character. Accordingly, ESR measurements on both displayed a broad spectrum both in solid state and in solution with  $g_e = 2.0017$  (Figure S2 in the Supporting Information). The VT ESR measurements on the powder disclosed that the ESR intensity decreased as the temperature decreased, indicating that both **DA-2Per-CN** and **DA-3Per-CN** have an open-shell singlet ground state.

The singlet–triplet energy gap  $\Delta E_{S-T}$  was estimated by SQUID measurements on the powder form of all samples at 5–380 K. The temperature-dependent magnetic susceptibility behavior was similar to that of most reported singlet diradicaloids; that is, the molar magnetic susceptibility increased with the temperature due to the thermal promotion of singlet species to triplet species (Figure 3 and Table 1). By carefully fitting the curves with the Bleaney–Bowers equation,<sup>22</sup> the  $\Delta E_{S-T}$  values were estimated to be −1.46 and −0.48 kJ/mol for **DA-2Per-CN** and **DA-3Per-CN**, respectively, indicating an increased diradical character with increasing chain length. The symmetric dimer **2Per-CN** and trimer **3Per-CN** have an estimated  $\Delta E_{S-T}$  value of −1.43 and −0.45 kJ/mol based on similar SQUID measurements and analysis,<sup>6c</sup> which are slightly smaller than the corresponding asymmetric dimer **DA-2Per-CN** and trimer **DA-3Per-CN**. That means the contribution of the diradical form to the ground state in the push–pull type systems is slightly smaller than that in the pull–pull type structures with the same conjugation length. This can be accounted for by the different energy required to break a

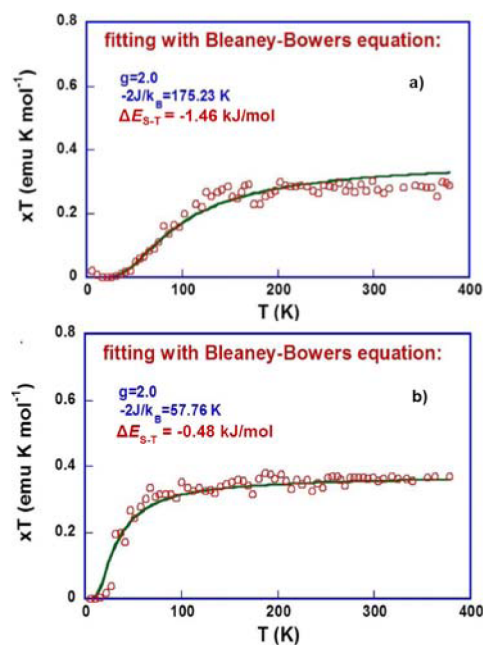


**Figure 3.**  $\chi T$ – $T$  curves in the SQUID measurements for the powder: (a) **DA-2Per-CN** and (b) **DA-3Per-CN**. The solid lines are the fitting curves according to Bleaney–Bowers equation;  $g$ -factor was taken to be 2.0.

double bond in a nonpolar (diradical) manner regarding that in a polar (zwitterionic) environment.

**2.3. X-ray Crystallographic Analysis.** The ground-state geometric structures of the push–pull and pull–pull type monomers **DA-Per-CN-b** and **Per-CN-b** were further characterized by X-ray crystallographic analyses. The single crystals of **DA-Per-CN-b** were obtained by slow evaporation of the solvent from the CHCl<sub>3</sub> solution, while the single crystals of **Per-CN-b** were grown from diffusion of methanol into the DCM solution.<sup>23</sup> Both of them adopted a slipped dimeric structure in an antiparallel packing mode with a short packing distance of ca. 3.31 Å through both dipole–dipole and  $\pi$ – $\pi$  interactions (Figure 4). Both molecules showed a bent perylene structure due to the fusion of five-membered ring at the bay region. The 2,6-dioctoxytolyl substituents are largely deviated from the NP plane, with a dihedral angle of 53.03° in **Per-CN-b** and 79.92° in **DA-Per-CN-b**. Because of the presence of bulky substitution, no continuously stacked columnar superstructure was observed. This accounts well for their good solubility and the observed sharp NMR/absorption spectra in solution. The **DA-Per-CN** molecule showed a longer central C=C double bond on the *N*-annulated five-membered ring (C10–C11, 1.352 Å) relative to the corresponding bond in **Per-CN-b** molecule (C6–C7, 1.345 Å). Other double bonds on the perylene unit in the asymmetric **DA-Per-CN-b** (C4–C9, 1.414 Å and C1–C2, 1.377 Å) were also found to be slightly longer than the same bond in the symmetric **Per-CN-b** (C11–C12, 1.411 Å/C4–C5, 1.412 Å and C1–C2, C8–C9, 1.363 Å). A similar trend was observed for external C=C double bond linking the NP unit and the two cyano- groups; that is, the symmetric **Per-CN-b** exhibited a shorter double bond length (C10–C24, 1.389 Å/C3–C21, 1.393 Å) than that in the asymmetric **DA-Per-CN-b** (C14–C21: 1.414 Å). This bond length analysis suggests that the zwitterionic resonance form contributes significantly to the ground state of the push–pull type **DA-Per-CN-b** molecule and drives the perylene unit to be

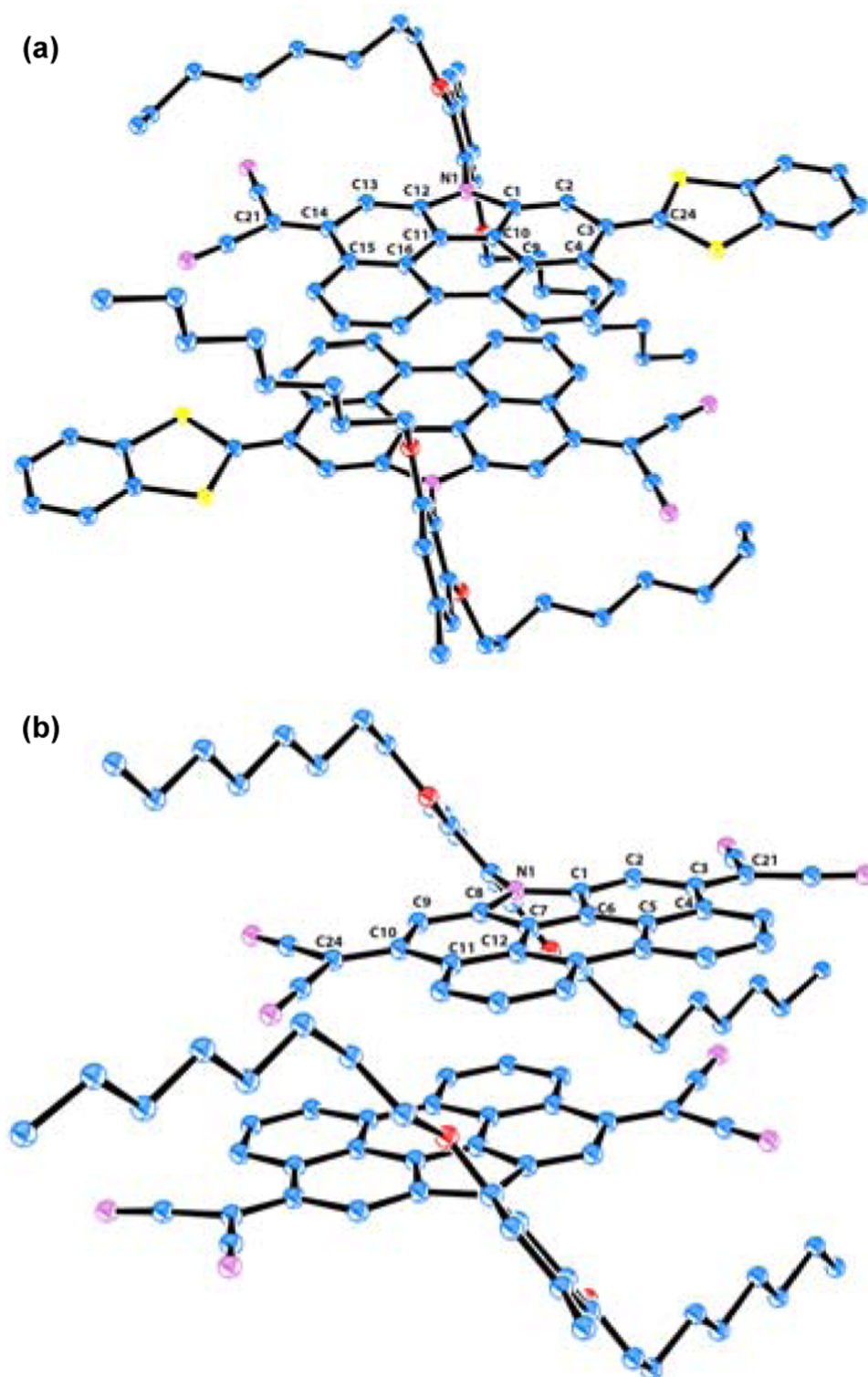


**Figure 4.** Single crystal structures of DA-Per-CN-b and Per-CN-b.

more aromatic than in the pull-pull type Per-CN-b. In addition, the  $\pi$ -conjugated framework along the long molecular axis shows a nearly planar geometry in both cases, indicating that the quinoidal form still contributes the most to the ground state, leading to a closed-shell ground state. In view of the 3D packing, besides a dimer structure formed by the next two D- $\pi$ -A molecules (up and down) as stated, the neighboring molecules in the same layer (left and right) show a head-to-tail

polymer chain via [C-H $\cdots$ N $\equiv$ C-] contacts (2.511 Å) likely arising from electrostatic interaction between the positive end (benzo-1,3-dithiol-2-ylidene) and the negative end (dicyano group) (Figure S3 in the Supporting Information). However, such a packing feature was not found in the pull-pull molecule Per-CN-b.

**2.4. Raman Characterizations.** Raman spectroscopy has been successfully used to describe the molecular structures of

the ground electronic states of pro-aromatic quinoidal compounds based on the sensitivity of the Raman bands from the quinoidal to aromatic structural transformation.<sup>24,6c-e</sup>

Figure 5 shows the Raman spectra of the three push–pull type

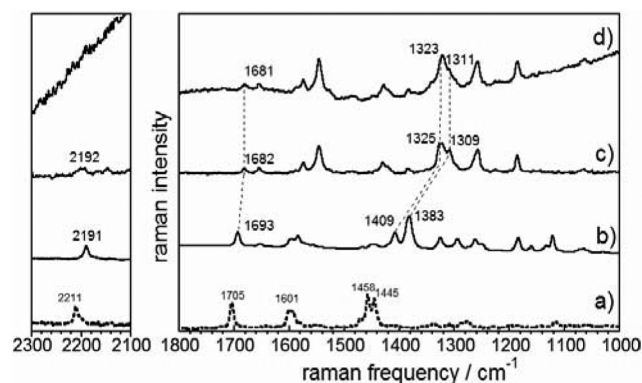


**Figure 5.** 633 nm Raman spectra in solid state of (a) Per-CN-a, (b) DA-Per-CN-a, (c) DA-2Per-CN, and (d) DA-3Per-CN obtained at  $-170\text{ }^{\circ}\text{C}$ .

perylene compounds (DA-Per-CN-a, DA-2Per-CN, and DA-3Per-CN) as compared to the pull–pull type monomer analogue Per-CN-a, which has been shown to possess a well-defined closed-shell quinoidal structure in its singlet ground electronic state, and the Raman spectrum gave high wavenumber values of its  $\nu(\text{C}\equiv\text{N})$  ( $2211\text{ cm}^{-1}$ ) and  $\nu(\text{C}=\text{C})$  vibrational bands ( $1705$  and  $1458\text{ cm}^{-1}$ ).<sup>6c</sup> As compared to Per-CN-a, compound DA-Per-CN-a disclosed a less quinoidal or more aromatic structure given the lower wavenumbers of its relevant bands at  $2191$ ,  $1693$ , and  $1400\text{--}1382\text{ cm}^{-1}$ , which originated from the enlargement of the  $\text{C}\equiv\text{N}$  and  $\text{C}=\text{C}$  double bond distances in the zwitterionic form as a result of the charge-transfer effect from the benzodithiol donor to the dicyanomethylene acceptor. A further wavenumber downshift from DA-Per-CN-a to DA-2Per-CN was observed in the

Raman spectra for the  $\nu(\text{C}=\text{C})$  bands to  $1682\text{ cm}^{-1}$  and  $1325\text{--}1310\text{ cm}^{-1}$ . This might indicate a further aromatization effect in the bis-NP bridge. However, as compared to the  $-20\text{ cm}^{-1}$  change on Per-CN-a to DA-Per-CN-a, there is almost no shift of the  $\nu(\text{C}\equiv\text{N})$  band from DA-Per-CN-a to DA-2Per-CN, indicating a decreasing effect of the push–pull contribution. This is reasonable because the donor–acceptor coupling is strongly mitigated by the donor to acceptor distance and it is only relevant in compounds with short bridges (e.g., the monomer), while in long-bridge donor–acceptor molecules this effect is rather local. In contrast, the wavenumber changes in the bridge  $\nu(\text{C}=\text{C})$  bands were of similar magnitude on that from Per-CN-a to DA-Per-CN-a and to DA-2Per-CN, meaning that the aromatization process is independent of the donor–acceptor coupling, which is in line with the appearance of an aromatic singlet diradical feature in the bridge superimposed with the donor–acceptor effect. This highlights a structural situation in which the donor–acceptor interaction is mainly operative at the terminal parts of the molecule, leaving the central moiety to develop the open-shell diradical shape. On passing from DA-2Per-CN to DA-3Per-CN, the Raman spectra did not significantly change, and both profiles became rather similar disclosing large diradical characters in the ground electronic state structure for higher series. In our push–pull type compounds, it seems that the open-shell diradical or a complete aromatic form is already fully established in DA-2Per-CN, which does not further increase in DA-3Per-CN, suggesting that the donor–acceptor and the diradical processes act together to aromatize the central bis-NP segment, but an additional NP unit in the bridge does not reinforce this effect. As compared to the Raman spectra of 2Per-CN and 3Per-CN, the spectrum of DA-2Per-CN is much more similar to that of 3Per-CN, which is in accordance with the above-mentioned comparison among their electronic absorption spectra, indicating aromatic character of the NP units in the DA-2Per-CN similar to that in 3Per-CN.

**2.5. TA and TPA Measurements.** The chain length-dependent excited-state dynamics and two-photon absorption

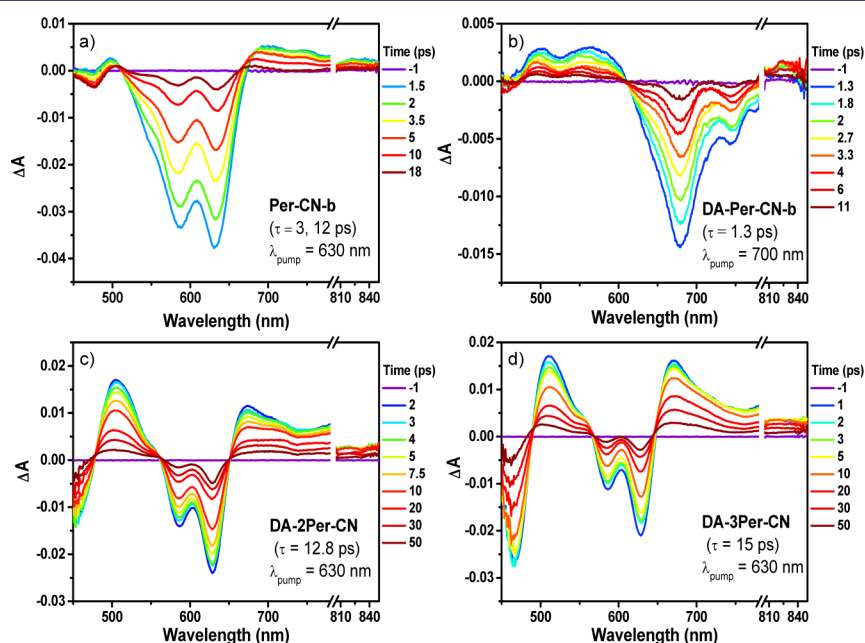


**Figure 6.** Transient absorption spectra of (a) Per-CN-b, (b) DA-Per-CN-b, (c) DA-2Per-CN, and (d) DA-3Per-CN recorded in toluene.

properties of these new push–pull type quinoidal NPs **DA-Per-CN-b** and **DA-*n*Per-CN** ( $n = 2,3$ ) were also investigated and compared to their corresponding pull–pull type analogous **Per-CN-b** and ***n*Per-CN**s ( $n = 2,3$ ). The femtosecond transient absorption spectra of **Per-CN-b**, **DA-Per-CN-b**, and **DA-*n*Per-CN** ( $n = 2, 3$ ) in toluene are shown in Figure 6. The TA spectrum of **Per-CN-b** exhibited a ground-state bleaching (GSB) signal around 585/631 nm, as well as a small excited-state absorption (ESA) band above 670 nm. The decay profiles probed at 630 nm were fitted by two exponential functions of 3 and 12 ps. In contrast, the push–pull monomer **DA-Per-CN-b** exhibited a different excited-state dynamics, with the appearance of an intense GSB band at 680/745 nm and a moderate ESA band at 460–610 nm spectral region. The short-wavelength ESA band may be correlated to the charge-separated species in the excited state. The singlet excited-state lifetime ( $\tau$ ) probed at 700 nm was determined as 1.3 ps, indicating a faster excited-state decay process than **Per-CN-b**, which could be correlated to its much smaller energy gap. The higher series **DA-2Per-CN** and **DA-3Per-CN** show similar TA spectra with a slight difference in their GSB and ESA band position and intensity, which also resemble that of the symmetric trimer **3Per-CN**.<sup>6c</sup> This is consistent with the similarity of their OPA spectra and can be explained by the similar aromatic character of the NP spacer. The  $\tau$  value was determined as 12.8 and 15.0 ps for **DA-2Per-CN** and **DA-3Per-CN**, respectively. Such a chain length dependence of  $\tau$  value in nonpolar toluene is in contrast to that observed for the symmetric oligomers ***n*Per-CN**s,<sup>6c</sup> but it is also dependent on solvent polarity as we will discuss in the next session.

In accordance with theoretical predictions,<sup>8</sup> many open-shell singlet diradicaloids with a moderate diradical character have demonstrated larger TPA activity as compared to closed-shell and pure diradicals.<sup>4,6,9</sup>

Nakano et al. also predicted that intramolecular charge transfer in a quadruple-type (D– $\pi$ –D or A– $\pi$ –A)<sup>25</sup> or a dipole-type (D– $\pi$ –A)<sup>16</sup> diradicaloid can further enhance the NLO response. In our cases, the ***n*Per-CN** series can be regarded as A– $\pi$ –A type quadrupolar chromophores, while the **DA-*n*Per-CN** series should belong to the D– $\pi$ –A type dipolar molecules. Therefore, it is of interest to compare the TPA activity of these two types of chromophores. TPA measurements were conducted by using the open-aperture Z-scan method in the NIR region where OPA contribution is negligible (Figure 2 and Table 1). As mentioned before, the **DA-Per-CN-b** carrying a bulky substituent can eliminate the long-wavelength absorption tail observed for the **DA-Per-CN-a**. For comparison, the symmetric monomer **Per-CN-b** carrying the same substituent was also measured. **DA-Per-CN-b** in DCM gave a maximum TPA cross-section value ( $\sigma_{\max}^{(2)}$ ) of about 1000 GM at 1500 nm, which is slightly smaller than the pull–pull type monomer **Per-CN-b** ( $\sigma_{\max}^{(2)} = 1200$  GM at 1200 nm under similar measurement conditions). Chromophores **DA-2Per-CN** and **DA-3Per-CN** in DCM gave similar  $\sigma_{\max}^{(2)}$  values of about 660 GM and 670 GM at 1900 nm, respectively, which are at the same level of symmetric higher series ***n*Per-CN** ( $n = 3–6$ ). However, both of them are smaller than the values for the monomer, again suggesting that too large diradical character does not benefit the NLO response. This observation also suggests that substitution of the extended *p*-QDMs in a symmetric A– $\pi$ –A or an asymmetric D– $\pi$ –A structure gives a similar effect on the TPA activity. Analogues with four methyl groups as substituents will be good references

for understanding the intramolecular charge transfer effect, which however turned out to be very unstable even for the monomer according to our preliminary experimental attempts.

**2.6. Electrochemical Properties.** Cyclic voltammetry and differential pulse voltammetry measurements were performed to investigate the electrochemical properties of these asymmetric oligomers (Figure S4 in the Supporting Information and Table 1). In contrast to the symmetric **Per-CN-b**, which only showed three reduction waves with half-wave potentials  $E_{1/2}^{\text{red}}$  at  $-0.54$ ,  $-0.78$ , and  $-1.38$  V (vs Fc/Fc<sup>+</sup>, Fc: ferrocene), the asymmetric **DA-Per-CN-b** exhibited two reversible oxidation waves with  $E_{1/2}^{\text{ox}}$  at 0.32 and 0.78 V and one chemically irreversible reductive wave with  $E_{1/2}^{\text{red}}$  at  $-1.02$  V. The HOMO and LUMO energy levels of **DA-Per-CN-b** were determined to be  $-5.06$  and  $-3.85$  eV, respectively, from the onset potentials of the first oxidation and reduction wave. **DA-2Per-CN** demonstrated three (quasi)reversible redox waves with oxidation waves at  $E_{1/2}^{\text{ox}} = 0.31$ , 0.47, and 0.83 V and one reversible reduction wave at  $E_{1/2}^{\text{red}} = -0.40$  V, together with two chemically irreversible reduction processes at  $E_{1/2}^{\text{red}} = -1.38$  and  $-1.12$  V. On passing to **DA-3Per-CN**, five closely overlapped oxidative processes with  $E_{1/2}^{\text{ox}}$  at 0.32, 0.49, 0.60, 0.76, 0.89 V were observed, together with three reductive processes with  $E_{1/2}^{\text{red}}$  at  $-1.40$ ,  $-1.16$ , and  $-0.40$  V. Accordingly, the HOMO and LUMO energy levels of **DA-2Per-CN** and **DA-3Per-CN** were estimated to be  $-5.06$ ,  $-4.46$  eV, and  $-5.02$ ,  $-4.52$  eV, respectively. Rather low electrochemical energy gaps were estimated for these three push–pull type oligomers as 1.21, 0.60, and 0.50 eV, respectively. Such chain length dependence of their electrochemical behavior provides important insights into the correlation between the change of  $\pi$ -conjugation and electronic structures in these extensive asymmetric homologues.

### 3. Solvent-Dependent Ground States and Physical Properties.

**3.1. One-Photon Absorption Spectra.** To explore the solvent effect on the nature of the electronic ground states and physical properties of these push–pull type chromophores, we conducted OPA measurements in solvents with increasing polarity from toluene to THF, to DCM, and to a mixed solvent system of 1:1 (v/v) DMSO/DCM, where at least 50% DCM should be added to make a clear solution. The asymmetric monomer **DA-Per-CN-b** displayed an obvious red shift of the absorption band with the increase of solvent polarity (Figure 7), which is a typical solvatochromic effect for many chromophores with significant intramolecular charge transfer character. At the same time, the relative intensity of the two

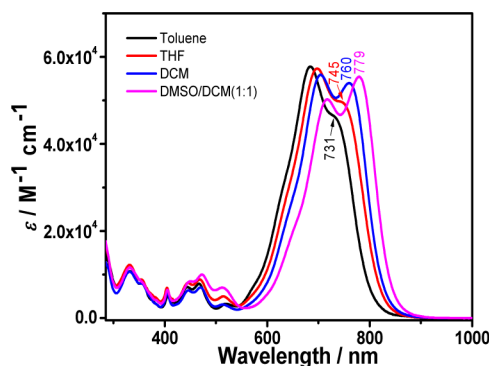


**Figure 7.** One-photon absorption spectra of **DA-Per-CN-b** in toluene, THF, DCM, and DMSO/DCM (1:1).



peaks in the major absorption band also changed, in which the relative intensity of the longer wavelength increases with the solvent polarity. These findings must be associated with the contribution of the aromatic zwitterionic resonance form to the ground state, which is reinforced when the solvent polarity is increased. In contrast, such a solvent-dependent spectral change was not observed for the pull–pull type **Per-CN-b** (Figure S5 in the Supporting Information). On passing to the higher asymmetric analogues **DA-2Per-CN** and **DA-3Per-CN**, the solvent dependence was not so obvious, and only in highly polar solvents, such as DMSO/DCM (1:1), did the absorption spectra show some observable band alteration (Figure S5 in the Supporting Information). This can be explained by their much larger diradical characters, and the contribution of the zwitterionic resonance form to the ground state is much less as compared to the push–pull monomer, which is in agreement with the ESR/SQUID and Raman data analysis.

**3.2. TA and TPA Spectra.** The solvent-dependent excited-state dynamics and TPA activities of these new push–pull type chromophores were also investigated considering the change of their ground-state electronic structures. TA/TPA measurements were conducted in solvents with different polarities, by using the same set of solvents as for the OPA measurements (Figures S6–18 in the Supporting Information).

Generally, there was no significant change in the TA spectra, but the singlet excited-state lifetimes showed obvious changes with the solvent polarity. With increase of the solvent polarity, the  $\tau$  value increases for **DA-Per-CN-b**, but decreases for higher series **DA-2Per-CN** and **DA-3Per-CN**, and there was no significant change for the symmetric **Per-CN-b** (Figure 8a). Such a difference should be associated with the more significant contribution of the zwitterion form for the asymmetric **DA-**

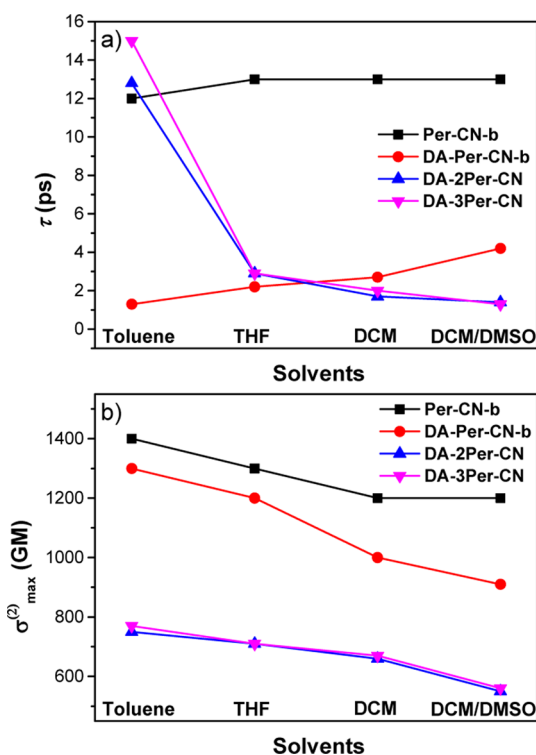


**Figure 8.** Solvent-dependent (a) singlet excited-state lifetime ( $\tau$ ) and (b) TPA cross section maximum ( $\sigma_{\max}^{(2)}$ ) of **Per-CN-b**, **DA-Per-CN-b**, **DA-2Per-CN**, and **DA-3Per-CN**.

**Per-CN-b** as compared to its dimer and trimer analogues and the symmetric monomer. The fundamental reasons for the increase/decrease of the singlet excited-state lifetime with the solvent polarity however could be complicated, and it is not so simple to conclude at this stage.

The TPA cross-section maxima of these push–pull chromophores and the pull–pull **Per-CN-b** displayed a common trend; that is, with the increase of the solvent polarity, the  $\sigma_{\max}^{(2)}$  value slightly decreased (Figure 8b). This finding suggests that the solvent has less effect on the TPA activity, and the variation of the  $\sigma_{\max}^{(2)}$  may rather come from the intrinsic solvent effect during the Z-scan measurements. When comparing these compounds in the same solvent, the  $\sigma_{\max}^{(2)}$  follows an order: **Per-CN-b** > **DA-Per-CN** > **DA-2Per-CN**  $\approx$  **DA-3Per-CN**. In DCM, the symmetric oligomers **nPer-CN**s ( $n = 1-3$ ) series<sup>6c</sup> have a slightly larger  $\sigma_{\max}^{(2)}$  value as compared to the corresponding asymmetric analogous, but there is no significant difference, suggesting that the D- $\pi$ -A and A- $\pi$ -A configurations have almost the same effect on their nonlinear optical response.

**4. Theoretical Calculations and Discussion.** To further understand the chain length dependence of the ground state and physical properties, we first investigate the diradical character of three quinoidal NP oligomer model systems: (1) A- $\pi$ -A type **A-n** ( $n = 1-3$ ), (2) D- $\pi$ -A type **B-n** ( $n = 1-3$ ), and (3) G- $\pi$ -G (G represents  $=C(CH_3)_2$  group) type **C-n** ( $n = 1-3$ ) (Figure 9). The alkyl or tolyl substituents at the amine

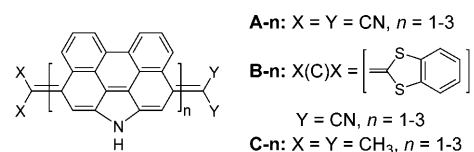


**Figure 9.** Model compounds used for DFT calculations.

site were replaced by hydrogen to reduce the computational cost. Geometry optimization for all of the model systems was carried out using the UB3LYP/6-311G\* method.

The optimized geometries of the NP monomers (**A-1** and **B-1**) were first compared to the crystallographic data of the corresponding **Per-CN-b** and **DA-Per-CN-b**, with the focus on the exoperylene C–C(CN)<sub>2</sub> bond length. On the basis of the resonance structures (Figure 1), the diradical and zwitterionic contributions should increase the C–C(CN)<sub>2</sub> bond lengths as compared to the standard double bond length. The calculated C–C(CN)<sub>2</sub> bond lengths are similar to the crystallographic data. Consistent with the experimental results, the asymmetric **B-1** exhibits a larger C–C(CN)<sub>2</sub> bond length (1.408 Å) than that of the symmetric **A-1** (1.399 Å), implying that the contribution of the quinoidal resonance structure is smaller in the asymmetric system than in the symmetric system.

The diradical character index  $y$  of the three model systems was calculated by a LC-UBLYP ( $\mu = 0.33$ )/6-311+G\* level of theory,<sup>26</sup> and the results are collected in Table 2. The major

**Table 2.** Calculated Diradical Characters ( $y$ ) of **A-n-C-n** ( $n = 1-3$ )

$y$	$n = 1$	$n = 2$	$n = 3$
<b>A-n</b>	0.150	0.913	0.994
<b>B-n</b>	0.123	0.899	0.995
<b>C-n</b>	0.004	0.933	0.996

findings include the following: (1) In all three systems, the monomer ( $n = 1$ ) exhibits a small  $y$  value (nearly closed-shell), although the dimer ( $n = 2$ ) and the trimer ( $n = 3$ ) show quite large  $y$  values (almost pure open-shell). This abrupt increase of  $y$  from monomer to dimer is likely to be caused by the large steric repulsion between the NP units in the rigid quinoidal structure, which tends to become a more flexible diradical/ionic form. In fact, large dihedral angles between the NP units were calculated for all three dimers ( $57.8^\circ$  for **A-2**,  $53.9^\circ$  for **B-2**, and  $59.9^\circ$  for **C2**). (2) From the comparison of the  $y$  values between the monomer of the two symmetric systems, it is found that the  $y$  of system **A-1** is larger than that of system **C-1**. This shows that the introduction of acceptor groups onto both ends of the open-shell systems increases the open-shell singlet nature, and this tendency was also observed in the previous study.<sup>27</sup> On the other hand, both dimers and trimers of **A- $n$**  and **C- $n$**  exhibit almost pure open-shell nature ( $y \approx 1$ ), which is hardly affected by the intramolecular charge transfer. (3) From the comparison of the  $y$  values between symmetric system **A- $n$**  and asymmetric system **B- $n$**  with the same conjugation length, it is found that the latter exhibits a slightly smaller  $y$  value due to the contribution of the zwitterionic form but there is no significant difference, indicating that **A- $\pi$ -A** and **D- $\pi$ -A** structures have a similar effect on their diradical characters in this special case. This is in accordance with the observed ESR/SQUID data.

Calculations also revealed that **B1–B3** all have a typical disjoint single occupied molecular orbital (SOMO) profile, indicating a singlet diradical ground state. Open-shell singlet nature can be also described with the spin-density distribution. In the strict sense, the spin-density distribution is an artifact for the open-shell singlet systems. However, it is known that the spin correlation between the different spins within multi-reference scheme is similar to the spin density of the unrestricted single reference scheme.<sup>28</sup> The spin densities are mainly distributed through the  $\pi$ -conjugated framework along the long axis in **B-1**, across both NP units in **B-2**, and localized on the terminal parts in **B-3** (Figure 10), indicating that the two spins interact less with each other with the increase in the chain length.

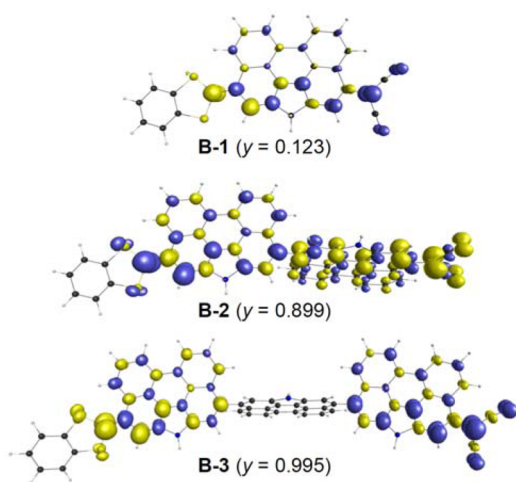


**Figure 10.** Spin density distributions in molecules **B1–B3** for their singlet diradical states. The yellow and blue surfaces represent  $\alpha$  and  $\beta$  spin density distributions with 0.005 au isosurfaces, respectively.

To evaluate the intramolecular charge transfer character in **B1–B3**, the Hirshfeld charges of the central NP units and the terminal regions were calculated (LC-UBLYP ( $\mu = 0.33$ )/6-311+G\*). It was found that all of the systems exhibit **D- $\pi$ -A** nature, and the strength gets smaller as the chain length become longer (Figure 11). This is probably due to two

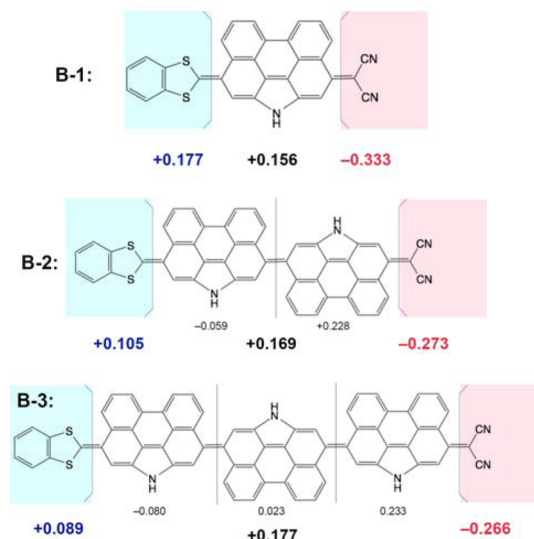


**Figure 11.** Calculated Hirshfeld charges of **B-1–B-3**.

reasons: one is simply that the distance between the **D** and **A** parts get larger, and the other is that the large dihedral angles between units decrease the effective  $\pi$ -conjugation length between units. In fact, looking at the effective charges of each NP unit in the **B-2** and **B-3**, the large part of the charge transfer occurs between the **D** or **A** moieties and the terminal NP units, and therefore large gaps of effective charges between the units within one system exist. Such calculations are in good agreement with all of the chain length and solvent-dependent physical measurements; that is, with extension of the chain length, the contribution of the zwitterion form decreases while the diradical character increases, and thus their physical properties become less solvent dependent.

### III. CONCLUSION

We have successfully synthesized a new series of push–pull type quinoidal perylene oligomers, which possess a unique ground-state electronic structure with a balanced contribution from a closed-shell quinoidal, an open-shell diradical, and a closed-shell zwitterionic resonance form. As a result, their ground states and physical properties were found to show a clear chain length and solvent polarity dependence, which were systematically investigated by various experiments and theoretical calculations. It was found that with extension of the chain length, the diradical character greatly increases, while the contribution of the zwitterionic form diminishes more and more. As a result, solvent polarity plays a major role in the ground state and physical properties of the monomer, but less on the dimer and trimer. By comparison with the symmetric **A- $\pi$ -A** analogous with similar conjugation length, these **D- $\pi$ -A** type chromophores exhibited similar diradical characters and TPA activities. To the best of our knowledge, our new system represents the first push–pull type extended  $p$ -QDM derivatives with an open-shell singlet diradical ground

state. It also provides guidance for the design of new chromophores with remarkable one-photon and two-photon properties in the future.

## ■ ASSOCIATED CONTENT

### Supporting Information

Synthetic procedures and characterization data of all other new compounds; details for all physical characterizations and theoretical calculations; additional spectroscopic and computational data. The Supporting Information is available free of charge on the ACS Publications website at DOI: 10.1021/jacs.5b04156.

## ■ AUTHOR INFORMATION

### Corresponding Authors

\*msedingj@nus.edu.sg

\*casado@uma.es

\*mnaka@cheng.es.osaka-u.ac.jp

\*dongho@yonsei.ac.kr

\*chmwuj@nus.edu.sg

### Notes

The authors declare no competing financial interest.

## ■ ACKNOWLEDGMENTS

J.W. acknowledges financial support from the MOE Tier 3 programme (MOE2014-T3-1-004) and MOE Tier 2 grant (MOE2014-T2-1-080). The work at Yonsei University was supported by Midcareer Researcher Program (NRF-2005-0093839) and Global Research Laboratory (2013K1A1A2A02050183) through the National Research Foundation of Korea (NRF) funded by the Ministry of Science, ICT (Information and Communication Technologies) and Future Planning. The work at the University of Málaga was supported by the Ministerio de Educación y Ciencia (MEC) of Spain and by FEDER funds (project CTQ2009-10098 and to the Junta de Andalucía for the research project PO9-4708). The work at Osaka University was supported by the Grant-in-Aid for Scientific Research (A) (no. 25248007) from Japan Society for the Promotion of Science (JSPS), and by the Grant-in-Aid for Scientific Research on Innovative Areas (“Stimuli-Responsive Chemical Species” (no. A24109002a), “ $\pi$ -System Figuration” (no. 15H00999), and “Photosynergetics” (no. A26107004a)), MEXT, Japan. Z.Z. is thankful for financial support from the Startup Fund (531109020043) from Hunan University.

## ■ REFERENCES

(1) (a) Rajca, A. *Chem. Rev.* **1994**, *94*, 871. (b) Morita, Y.; Suzuki, K.; Sato, S.; Takui, T. *Nat. Chem.* **2011**, *3*, 197. (c) Sun, Z.; Ye, Q.; Chi, C.; Wu, J. *Chem. Soc. Rev.* **2012**, *41*, 7857. (d) Shimizu, A.; Hirao, Y.; Kubo, T.; Nakano, M.; Botek, E.; Champagne, B. *AIP Conf. Proc.* **2012**, *1504*, 399. (e) Sun, Z.; Zeng, Z.; Wu, J. *Chem.—Asian J.* **2013**, *8*, 2894. (f) Abe, M. *Chem. Rev.* **2013**, *113*, 7011. (g) Sun, Z.; Zeng, Z.; Wu, J. *Acc. Chem. Res.* **2014**, *47*, 2582. (h) Kubo, T. *Chem. Rev.* **2015**, *15*, 218. (i) Zeng, Z.; Shi, X. L.; Chi, C.; López Navarrete, J. T.; Casado, J.; Wu, J. *Chem. Soc. Rev.* **2015**, DOI: 10.1039/c5cs00051c. (2) (a) Chikamatsu, M.; Mikami, T.; Chisaka, J.; Yoshida, Y.; Azumi, R.; Yase, K. *Appl. Phys. Lett.* **2007**, *91*, 043506. (b) Chase, D. T.; Fix, A. G.; Kang, S. J.; Rose, B. D.; Weber, C. D.; Zhong, Y.; Zakharov, L. N.; Lonergan, M. C.; Nuckolls, C.; Haley, M. M. *J. Am. Chem. Soc.* **2012**, *134*, 10349. (c) Kamada, K.; Ohta, K.; Kubo, T.; Shimizu, A.; Morita, Y.; Nakasuji, K.; Kishi, R.; Ohta, S.; Furukawa, S. I.; Takahashi, H.; Nakano, M. *Angew. Chem., Int. Ed.* **2007**, *46*, 3544. (d) Son, Y. W.; Cohen, M. L.; Louie, S. G. *Phys. Rev. Lett.* **2006**, *97*, 216803.

(e) Morita, Y.; Nishida, S.; Murata, T.; Moriguchi, M.; Ueda, A.; Satoh, M.; Arifuku, K.; Sato, K.; Takui, T. *Nat. Mater.* **2011**, *10*, 947.

(3) (a) Ohashi, K.; Kubo, T.; Masui, T.; Yamamoto, K.; Nakasuji, K.; Takui, T.; Kai, Y.; Murata, I. *J. Am. Chem. Soc.* **1998**, *120*, 2018. (b) Kubo, T.; Sakamoto, M.; Akabane, M.; Fujiwara, Y.; Yamamoto, K.; Akita, M.; Inoue, K.; Takui, T.; Nakasuji, K. *Angew. Chem., Int. Ed.* **2004**, *43*, 6474. (c) Kubo, T.; Shimizu, A.; Sakamoto, M.; Uruichi, M.; Yakushi, K.; Nakano, M.; Shiomi, D.; Sato, K.; Takui, T.; Morita, Y.; Nakasuji, K. *Angew. Chem., Int. Ed.* **2005**, *44*, 6564. (d) Shimizu, A.; Uruichi, M.; Yakushi, K.; Matsuzaki, H.; Okamoto, H.; Nakano, M.; Hirao, Y.; Matsumoto, K.; Kurata, H.; Kubo, T. *Angew. Chem., Int. Ed.* **2009**, *48*, 5482. (e) Shimizu, A.; Kubo, T.; Uruichi, M.; Yakushi, K.; Nakano, M.; Shiomi, D.; Sato, K.; Takui, T.; Hirao, Y.; Matsumoto, K.; Kurata, H.; Morita, Y.; Nakasuji, K. *J. Am. Chem. Soc.* **2010**, *132*, 14421. (f) Shimizu, A.; Hirao, Y.; Matsumoto, K.; Kurata, H.; Kubo, T.; Uruichi, M.; Yakushi, K. *Chem. Commun.* **2012**, *48*, 5629.

(4) (a) Umeda, R.; Hibi, D.; Miki, K.; Tobe, Y. *Org. Lett.* **2009**, *11*, 4104. (b) Wu, T. C.; Chen, C. H.; Hibi, D.; Shimizu, A.; Tobe, Y.; Wu, Y. T. *Angew. Chem., Int. Ed.* **2010**, *49*, 7059. (c) Sun, Z.; Huang, K.-W.; Wu, J. *Org. Lett.* **2010**, *12*, 4690. (d) Sun, Z.; Huang, K.-W.; Wu, J. *J. Am. Chem. Soc.* **2011**, *133*, 11896. (e) Li, Y.; Heng, W.-K.; Lee, B. S.; Aratani, N.; Zafra, J. L.; Bao, N.; Lee, R.; Sung, Y. M.; Sun, Z.; Huang, K.-W.; Webster, R. D.; López Navarrete, J. T.; Kim, D.; Osuka, A.; Casado, J.; Ding, J.; Wu, J. *J. Am. Chem. Soc.* **2012**, *134*, 14913. (f) Zeng, W.; Ishida, M.; Lee, S.; Sung, Y.; Zeng, Z.; Ni, Y.; Chi, C.; Kim, D.-H.; Wu, J. *Chem.—Eur. J.* **2013**, *19*, 16814. (g) Sun, Z.; Lee, S.; Park, K.; Zhu, X.; Zhang, W.; Zheng, B.; Hu, P.; Zeng, Z.; Das, S.; Li, Y.; Chi, C.; Li, R.; Huang, K.; Ding, J.; Kim, D.; Wu, J. *J. Am. Chem. Soc.* **2013**, *135*, 18229. (h) Sun, Z.; Wu, J. *J. Org. Chem.* **2013**, *78*, 9032. (i) Shan, L.; Liang, Z.-X.; Xu, X.-M.; Tang, Q.; Miao, Q. *Chem. Sci.* **2013**, *4*, 3294. (j) Zafra, J. L.; González Cano, R. C.; Delgado, M. C. R.; Sun, Z.; Li, Y.; López Navarrete, J. T.; Wu, J.; Casado, J. *J. Chem. Phys.* **2014**, *140*, 054706. (k) Li, Y.; Huang, K.-W.; Sun, Z.; Webster, R. D.; Zeng, Z.; Zeng, W. D.; Chi, C.; Furukawa, K.; Wu, J. *Chem. Sci.* **2014**, *5*, 1908. (l) Das, S.; Lee, S.; Son, M.; Zhu, X.; Zhang, W.; Zheng, B.; Hu, P.; Zeng, Z.; Sun, Z.; Zeng, W.; Li, R.-W.; Huang, K.-W.; Ding, J.; Kim, D.; Wu, J. *Chem.—Eur. J.* **2014**, *20*, 11410. (m) Sun, Z.; Zheng, B.; Hu, P.; Huang, K.-W.; Wu, J. *ChemPlusChem* **2014**, *79*, 1549.

(5) (a) Chase, D. T.; Rose, B. D.; McClintock, S. P.; Zakharov, L. N.; Haley, M. M. *Angew. Chem., Int. Ed.* **2011**, *50*, 1127. (b) Shimizu, A.; Tobe, Y. *Angew. Chem., Int. Ed.* **2011**, *50*, 6906. (c) Fix, A. G.; Deal, P. E.; Vonnegut, C. L.; Rose, B. D.; Zakharov, L. N.; Haley, M. M. *Org. Lett.* **2013**, *15*, 1362. (d) Rose, B. D.; Vonnegut, C. L.; Zakharov, L. N.; Haley, M. M. *Org. Lett.* **2013**, *14*, 2426. (e) Shimizu, A.; Kishi, R.; Nakano, M.; Shiomi, D.; Sato, K.; Takui, T.; Hisaki, I.; Miyata, M.; Tobe, Y. *Angew. Chem., Int. Ed.* **2013**, *52*, 6076. (f) Fix, A. G.; Chase, D. T.; Haley, M. M. *Top. Curr. Chem.* **2014**, *349*, 159. (g) Miyoshi, H.; Nobusue, S.; Shimizu, A.; Hisaki, I.; Miyatab, M.; Tobe, Y. *Chem. Sci.* **2014**, *5*, 163. (h) Young, B. S.; Chase, D. T.; Marshall, J. L.; Vonnegut, C. L.; Zakharov, L. N.; Haley, M. M. *Chem. Sci.* **2014**, *5*, 1008. (i) Luo, D.; Lee, S.; Zheng, B.; Sun, Z.; Zeng, W.; Huang, K.-W.; Furukawa, K.; Kim, D.; Webster, R. D.; Wu, J. *Chem. Sci.* **2014**, *5*, 4944.

(6) (a) Zhu, X.; Tsuji, H.; Nakabayashi, H.; Ohkoshi, S.; Nakamura, E. *J. Am. Chem. Soc.* **2011**, *133*, 16342. (b) Zeng, Z.; Sung, Y. M.; Bao, N.; Tan, D.; Lee, R.; Zafra, J. L.; Lee, B. S.; Ishida, M.; Ding, J.; López Navarrete, J. T.; Li, Y.; Zeng, W.; Kim, D.; Huang, K.-W.; Webster, R. D.; Casado, J.; Wu, J. *J. Am. Chem. Soc.* **2012**, *134*, 14513. (c) Zeng, Z.; Ishida, M.; Zafra, J. L.; Zhu, X.; Sung, Y. M.; Bao, N.; Webster, R. D.; Lee, B. S.; Li, R.-W.; Zeng, W.; Li, Y.; Chi, C.; López Navarrete, J. T.; Ding, J.; Casado, J.; Kim, D.; Wu, J. *J. Am. Chem. Soc.* **2013**, *135*, 6363. (d) Zeng, Z.; Lee, S.; Zafra, J. L.; Ishida, M.; Zhu, X.; Sun, Z.; Ni, Y.; Webster, R. D.; Li, R.-W.; López Navarrete, J. T.; Chi, C.; Ding, J.; Casado, J.; Kim, D.; Wu, J. *Angew. Chem., Int. Ed.* **2013**, *52*, 8561. (e) Zeng, Z.; Lee, S.; Zafra, J. L.; Ishida, M.; Bao, N.; Webster, R. D.; López Navarrete, J. T.; Ding, J.; Casado, J.; Kim, D.-H.; Wu, J. *Chem. Sci.* **2014**, *5*, 3072. (f) Zeng, Z.; Wu, J. *Chem. Rev.* **2015**, *15*, 322.

(7) (a) Konishi, A.; Hirao, Y.; Nakano, M.; Shimizu, A.; Botek, E.; Champagne, B.; Shiomi, D.; Sato, K.; Takui, T.; Matsumoto, K.;

- Kurata, H.; Kubo, T. *J. Am. Chem. Soc.* **2010**, *132*, 11021. (b) Konishi, A.; Hirao, Y.; Matsumoto, K.; Kurata, H.; Kishi, R.; Shigeta, Y.; Nakano, M.; Tokunaga, K.; Kamada, K.; Kubo, T. *J. Am. Chem. Soc.* **2013**, *135*, 1430.
- (8) (a) Nakano, M.; Nagao, H.; Yamaguchi, K. *Phys. Rev. A* **1997**, *55*, 1503. (b) Nakano, M.; Kishi, R.; Nitta, T.; Kubo, T.; Nakasuji, K.; Kamada, K.; Ohta, K.; Champagne, B.; Botek, E.; Yamaguchi, K. *J. Phys. Chem. A* **2005**, *109*, 885. (c) Nakano, M.; Kubo, T.; Kamada, K.; Ohta, K.; Kishi, R.; Ohta, S.; Nakagawa, N.; Takahashi, H.; Furukawa, S.; Morita, Y.; Nakasuji, K.; Yamaguchi, K. *Chem. Phys. Lett.* **2006**, *418*, 142. (d) Ohta, S.; Nakano, M.; Kubo, K.; Kamada, K.; Ohta, K.; Kishi, R.; Nakagawa, N.; Champagne, B.; Botek, E.; Takebe, A.; Umezaki, S.; Nate, M.; Takahashi, H.; Furukawa, S.; Morita, Y.; Nakasuji, K.; Yamaguchi, K. *J. Phys. Chem. A* **2007**, *111*, 3633. (e) Nakano, M.; Kishi, R.; Takebe, A.; Nate, M.; Takahashi, H.; Kubo, T.; Kamada, K.; Ohta, K.; Champagne, B.; Botek, E. *Comput. Lett.* **2007**, *3*, 333. (f) Nakano, M.; Kishi, R.; Ohta, S.; Takahashi, H.; Kubo, T.; Kamada, K.; Ohta, K.; Botek, E.; Champagne, B. *Phys. Rev. Lett.* **2007**, *99*, 033001. (g) Nakano, M.; Nagai, H.; Fukui, H.; Yoneda, K.; Kishi, R.; Takahashi, H.; Shimizu, A.; Kubo, T.; Kamada, K.; Ohta, K.; Champagne, B.; Botek, E. *Chem. Phys. Lett.* **2008**, *467*, 120. (h) Yoneda, K.; Nakano, M.; Inoue, Y.; Inui, T.; Fukuda, K.; Shigeta, Y.; Kubo, T.; Champagne, B. *J. Phys. Chem. C* **2012**, *116*, 17787. (i) Nakano, M.; Champagne, B. *Theor. Chem. Acc.* **2015**, *134*, 23–1–9. (j) Nakano, M. *Excitation Energies and Properties of Open-Shell Singlet Molecules*; Springer: Cham, Heidelberg, New York, Dordrecht, London, 2014.
- (9) (a) Kamada, K.; Fuku-en, S.; Minamide, S.; Ohta, K.; Kishi, R.; Nakano, M.; Matsuzaki, H.; Okamoto, H.; Higashikawa, H.; Inoue, K.; Kojima, S.; Yamamoto, Y. *J. Am. Chem. Soc.* **2013**, *135*, 232. (b) Kishida, H.; Hibino, K.; Nakamura, A.; Kato, D.; Abe, J. *Thin Solid Films* **2010**, *519*, 1028. (c) Takauji, K.; Suizu, R.; Awaga, K.; Kishida, H.; Nakamura, A. *J. Phys. Chem. C* **2014**, *118*, 4303.
- (10) (a) Coulson, C. A.; Craig, D. P.; Maccoll, A.; Pullman, A. *Discuss. Faraday Soc.* **1947**, *2*, 36. (b) Szwarc, M. *Discuss. Faraday Soc.* **1947**, *2*, 46. (c) Hush, N. S. *J. Polym. Sci.* **1952**, *11*, 289.
- (11) (a) Thiele, J.; Balhorn, H. *Chem. Ber.* **1904**, *37*, 1463. (b) Flynn, C. R.; Michl, J. *J. Am. Chem. Soc.* **1974**, *96*, 3280.
- (12) (a) Tschitschibabin, A. E. *Chem. Ber.* **1907**, *40*, 1810. (b) Sloan, G. J.; Vaughan, W. R. *J. Org. Chem.* **1957**, *22*, 750. (c) Morozova, D. I.; Dyatkina, E. M. *Russ. Chem. Rev.* **1968**, *37*, 377. (d) Montgomery, L. K.; Huffman, J. C.; Jurczak, E. A.; Grendze, M. P. *J. Am. Chem. Soc.* **1986**, *108*, 6004. (e) Porter, W. W., III; Vaid, T. P.; Rheingold, A. L. *J. Am. Chem. Soc.* **2005**, *127*, 16559.
- (13) Acker, D. S.; Hertler, W. R. *J. Am. Chem. Soc.* **1962**, *84*, 3370.
- (14) (a) Hartzler, H. D. *J. Am. Chem. Soc.* **1964**, *86*, 2174. (b) Addison, A. W.; Dalal, N. S.; Hoyano, Y.; Huizinga, S.; Weiler, L. *Can. J. Chem.* **1977**, *55*, 4191. (c) Maxfield, M.; Bloch, A. N.; Cowan, D. O. *J. Org. Chem.* **1985**, *50*, 1789.
- (15) (a) Gronowitz, S.; Uppström, B. *Acta Chem. Scand., Ser. B* **1974**, *28*, 981. (b) Fukushima, T.; Okazeri, N.; Miyashi, T.; Suzuki, K.; Yamashita, Y.; Suzuki, T. *Tetrahedron Lett.* **1999**, *40*, 1175. (c) Suzuki, K.; Tomura, M.; Tanaka, S.; Yamashita, Y. *Tetrahedron Lett.* **2000**, *41*, 8359. (d) Pappenfus, T. M.; Chesterfield, R. J.; Frisbie, C. D.; Mann, K. R.; Casado, J.; Raff, J. D.; Miller, L. L. *J. Am. Chem. Soc.* **2002**, *124*, 4184. (e) Chesterfield, R. J.; Newman, C. R.; Pappenfus, T. M.; Ewbank, P. C.; Haukaas, M. H.; Mann, K. R.; Miller, L. L.; Frisbie, C. D. *Adv. Mater.* **2003**, *15*, 1278. (f) Takahashi, T.; Matsuoka, K. I.; Takimiya, K.; Otsubo, T.; Aso, Y. *J. Am. Chem. Soc.* **2005**, *127*, 8928. (g) Wu, Q.; Li, R.; Hong, W.; Li, H.; Gao, X.; Zhu, D. *Chem. Mater.* **2011**, *23*, 3138. (h) Casado, J.; Ortiz, R. P.; López Navarrete, J. T. *Chem. Soc. Rev.* **2012**, *41*, 5672. (i) Rudebusch, G. E.; Fix, A. G.; Henthorn, H. A.; Vonnegut, C. L.; Zakharov, L. N.; Haley, M. M. *Chem. Sci.* **2014**, *5*, 3627. (j) Shi, X.; Burrezo, P. M.; Lee, S.; Zhang, W.; Zheng, B.; Dai, G.; Chang, J.; López Navarrete, J. T.; Huang, K.-W.; Kim, D.; Casado, J.; Chi, C. *Chem. Sci.* **2014**, *5*, 4490.
- (16) (a) Nakano, M.; Minami, T.; Yoneda, K.; Muhammad, S.; Kishi, R.; Shigeta, Y.; Kubo, K.; Rougier, L.; Champagne, B.; Kamada, K.; Ohta, K. *J. Phys. Chem. Lett.* **2011**, *2*, 1094. (b) Nakano, M.; Champagne, B. *J. Chem. Phys.* **2013**, *138*, 244306.
- (17) Gompper, R.; Wagner, H.-U.; Kutter, E. *Chem. Ber.* **1968**, *101*, 4123–4143.
- (18) Inoue, S.; Aso, Y.; Otsubo, T. *Chem. Commun.* **1997**, 1105.
- (19) (a) Marder, S. R.; Gorman, C. B.; Tiemann, B. G.; Cheng, L. T. *J. Am. Chem. Soc.* **1993**, *115*, 3006. (b) Marder, S. R.; Cheng, L. T.; Tiemann, B. G.; Friedli, A. C.; Blanchard-Desce, M.; Perry, J. W.; Skindhoj, J. *Science* **1994**, *263*, 511. (c) Varanasi, P. R.; Jen, A. K.-Y.; Chandrasekhar, J.; Namboothiri, I. N. N.; Rathna, A. *J. Am. Chem. Soc.* **1996**, *118*, 12443. (d) Wang, Y.-K.; Shu, C.-F.; Breitung, E. M.; McMahon, R. J. *J. Mater. Chem.* **1999**, *9*, 1449. (e) Beckmann, S.; Etzbach, K.-H.; Krämer, P.; Lukaszuk, K.; Matschiner, R.; Schmidt, A. J.; Schuhmacher, P.; Sens, R.; Seybold, G.; Wortmann, R.; Würthner, F. *Adv. Mater.* **1999**, *11*, 536. (f) Breitung, E. M.; Shu, C.-F.; McMahon, R. J. *J. Am. Chem. Soc.* **2000**, *122*, 1154. (g) Milián, B.; Ortí, E.; Hernández, V.; Navarrete, J. T. L.; Otsubo, T. *J. Phys. Chem. B* **2003**, *107*, 12175. (h) Smith, M. J.; Clegg, W.; Nguyen, K. A.; Rogers, J. E.; Pachter, R.; Fleitz, P. A.; Anderson, H. L. *Chem. Commun.* **2005**, 2433. (i) Takahashi, T.; Takimiya, K.; Otsubo, T.; Aso, Y. *Org. Lett.* **2005**, *7*, 4313. (j) Ma, X.; Ma, F.; Zhao, Z.; Song, N.; Zhang, J. *J. Mater. Chem.* **2009**, *19*, 2975. (k) Ma, X.; Ma, F.; Zhao, Z.; Song, N.; Zhang, J. *J. Mater. Chem.* **2010**, *20*, 2369. (l) Andreu, R.; Galán, E.; Orduna, J.; Villacampa, B.; Alicante, R.; López Navarrete, J. T.; Casado, J.; Garín, J. *Chem.—Eur. J.* **2011**, *17*, 826–838. (m) Martínez de Baroja, N.; Garín, J.; Orduna, J.; Andreu, R.; Blesa, M. J.; Villacampa, B.; Alicante, R.; Franco, S. *J. Org. Chem.* **2012**, *77*, 4634.
- (20) Uno, M.; Seto, K.; Masuda, M.; Ueda, W.; Takahashi, S. *Tetrahedron Lett.* **1985**, *26*, 1553.
- (21) Qi, Q.; Wang, X.; Fan, L.; Zheng, B.; Zeng, W.; Luo, J.; Huang, K.; Wang, Q.; Wu, J. *Org. Lett.* **2015**, *17*, 724.
- (22) Bleaney, B.; Bowers, K. D. *Proc. R. Soc. London, Ser. A* **1952**, *214*, 451.
- (23) (a) Crystallographic data for **Per-CN-b** (100 K):  $C_{49}H_{47}N_5O_2$ ,  $M_w = 737.91$ ; monoclinic; space group  $P2_1/n$ ;  $a = 17.8586(13)$  Å,  $b = 8.3703(6)$  Å,  $c = 26.813(2)$  Å,  $\alpha = 90^\circ$ ,  $\beta = 96.883(4)^\circ$ ,  $\gamma = 90^\circ$ ;  $V = 3979.2(5)$  Å<sup>3</sup>;  $Z = 4$ ;  $\rho_{\text{calcd}} = 1.232$  Mg/m<sup>3</sup>;  $R_1 = 0.0553$ ,  $wR_2 = 0.1325$  ( $I > 2\sigma(I)$ );  $R_1 = 0.0821$ ,  $wR_2 = 0.1481$  (all data). (b) Crystallographic data for **DA-Per-CN-b** (100 K):  $C_{53}H_{51}N_3O_2S_2$ ,  $M_w = 826.08$ ; triclinic; space group  $P\bar{1}$ ;  $a = 9.2392(4)$  Å,  $b = 15.2056(6)$  Å,  $c = 15.3450(6)$  Å,  $\alpha = 94.7350(18)^\circ$ ,  $\beta = 105.0450(18)^\circ$ ,  $\gamma = 94.6510(18)^\circ$ ;  $V = 2062.98(15)$  Å<sup>3</sup>;  $Z = 2$ ;  $\rho_{\text{calcd}} = 1.330$  Mg/m<sup>3</sup>;  $R_1 = 0.0443$ ,  $wR_2 = 0.1098$  ( $I > 2\sigma(I)$ );  $R_1 = 0.0590$ ,  $wR_2 = 0.1190$  (all data).
- (24) (a) Ortiz, R. P.; Casado, J.; Gonzalez, S. R.; Hernandez, V.; Ortiz, R. P.; Casado, J.; Hernandez, V.; Navarrete, J. T. L.; Viruela, P. M.; Ortí, E.; Takimiya, K.; Otsubo, T. *Angew. Chem., Int. Ed.* **2007**, *46*, 9057. (b) Casado, J.; Patchkovskii, S.; Zgierski, M. Z.; Hermosilla, L.; Sieiro, C.; Moreno Oliva, M.; López Navarrete, J. T. *Angew. Chem., Int. Ed.* **2008**, *47*, 1443. (c) González, S. R.; Ie, Y.; Aso, Y.; López Navarrete, J. T.; Casado, J. *J. Am. Chem. Soc.* **2011**, *133*, 16350.
- (25) Fukuda, K.; Nakano, M. *J. Phys. Chem. A* **2014**, *118*, 3463.
- (26) Yamaguchi, K. *Chem. Phys. Lett.* **1975**, *33*, 330.
- (27) Kishi, R.; Dennis, M.; Fukuda, K.; Murata, Y.; Morita, K.; Uenaka, H.; Nakano, M. *J. Phys. Chem. C* **2013**, *117*, 21498.
- (28) Plasser, F.; Pašalić, H.; Gerzabek, M. H.; Libisch, F.; Reiter, R.; Burgdrcfer, J.; Müller, T.; Shepard, R.; Lischka, H. *Angew. Chem., Int. Ed.* **2013**, *52*, 2581.